ACS APPLIED MATERIALS & INTERFACES

Research Article

www.acsami.org

Redox-Functionalized Graphene Oxide Architecture for the Development of Amperometric Biosensing Platform

Ramendra Sundar Dey and C. Retna Raj*

Department of Chemistry, Indian Institute of Technology, Kharagpur 721302, India

Supporting Information

ABSTRACT: We describe the redox functionalization of graphene oxide (GO) and the development of versatile amperometric biosensing platforms for clinically important analytes such as cholesterol ester, uric acid and glucose. Ferrocene (Fc) redox units were covalently tethered onto the GO backbone using diamine sigma spacers of different chain lengths (C3-, C6-, and C9-diamines). The functionalized GO (Fc-GO) displays a pair of redox peak corresponding to Fc/Fc^+ redox couple at ~0.225 V. The surface coverage and heterogeneous electron transfer rate constant of Fc-GO depends on the length of sigma spacer. Amperometric biosensors for cholesterol (total), uric acid and glucose have been developed by integrating Fc-GO and the respective redox enzymes with screen printed electrode. Fc-GO efficiently mediates the bioelectrocatalytic oxidation of the substrates in the presence of the redox enzymes. The spacer length of Fc-GO controls the bioelectrocatalytic response of the biosensing platforms. The sensitivity of the biosensors based on C9 sigma spacer is significantly higher than the others. The detection limit (S/N = 3) of the biosensors for cholesterol and uric acid was 0.1 μM and for glucose it was 1 μM. Excellent stability, reproducibility, selectivity and fast response time were achieved. Biosensing of cholesterol, uric acid and glucose in human serum sample is successfully demonstrated with the biosensors, and the results are validated with the clinical laboratory measurement.

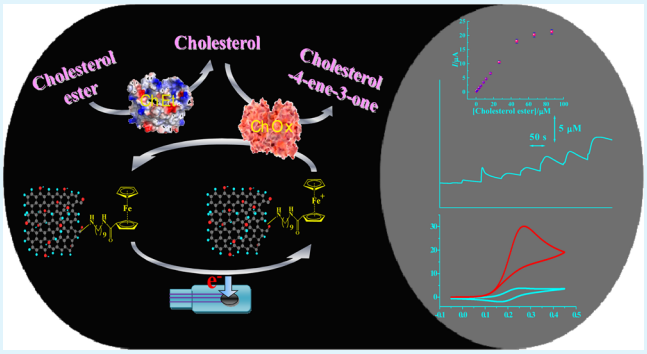

KEYWORDS: *functionalized graphene oxide, ferrocene, amperometric biosensor, cholesterol, glucose, uric acid*

INTRODUCTION

The control and management of the clinical analytes like cholesterol, uric acid, and glucose levels in human fluids is very essential to have a healthy life. It is known that the abnormal levels of these analytes in blood cause life threatening diseases. Globally, diabetes is one of the major causes for death and disability and more than 4 millions of people are dying every year due to complications associated with abnormal blood glucose level.[1] The diagnosis and management of diabetes requires highly sensitive reliable biosensors for the rapid and accurate measurement of blood glucose. On the other hand, the undesirable accumulation of cholesterol on the walls of arteries leads to the formation of atherosclerotic plaque and blocks the proper flow of blood. The level of total cholesterol in serum is an indicator in the diagnosis and prevention of heart diseases. The normal level of total cholesterol in serum is 200 mg/dL and its elevated level is a serious concern.[2] Uric acid is an end product of purine metabolism and the abnormal concentration of uric acid cause gout, arthritis, hypertension, etc.[3,4] Development of inexpensive electrochemical sensors/biosensors for the sensing of these analytes is in high demand in clinical practices. For practical applications, the electrochemical sensors/biosensors should have high sensitivity, good selectivity, and fast response time. Several approaches based on redox mediators, nanomaterials, redox enzymes, etc., have been developed in the past.[5−15] The electrochemical biosensors based on artificial electron acceptors are very promising and have many advantages over the conventional first generation biosensors. The soluble mediators with low redox potential and good stability can effectively communicate with the redox center of the enzyme and decrease the overpotential and mitigate the interference due to other electroactive analytes. The organic and metal−organic mediators such as osmium and ruthenium complexes, ferrocene derivatives, methyl viologen, etc., have been employed for the development of a mediator-based biosensor.[16−33] For instance, Turner's group has demonstrated the use of ferrocene-based mediators in the biosensing of glucose.[25] Schmidtke's group has extensively worked on a glucose biosensor based on ferrocene-modified linear polymer film.[26,27] Qiu's group has proposed a one-step fabrication of a glucose biosensor by in situ codeposition of ferrocene-branched chitosan, MWCNT, and glucose oxidase on the electrode surface.[28] Mannino's group has reported a polyamide nanofibrous membrane-based glucose biosensor where ferrocene methanol is employed as the mediator.[29] Heller's group has pioneered the development of blood-glucose strips using

Received: January 22, 2013
Accepted: May 17, 2013
Published: May 30, 2013

   dx.doi.org/10.1021/am400280u | ACS Appl. Mater. Interfaces 2013, 5, 4791−4798

Scheme 1. Scheme Illustrating the Functionalization of GO Sheets by Ferrocene Units

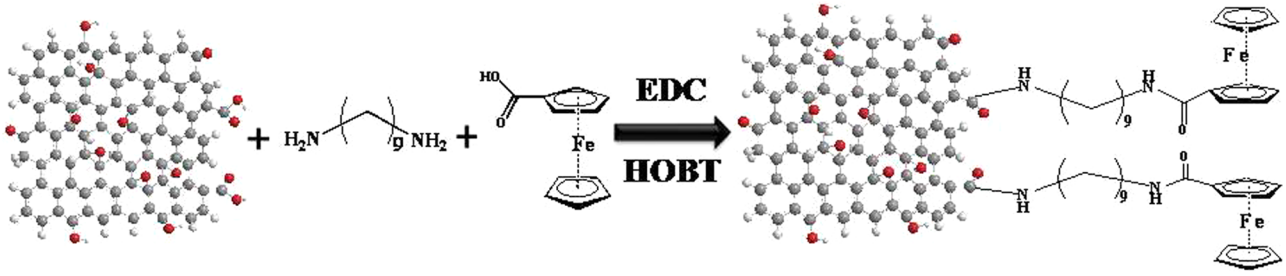

osmium-based complex.[16,17] Recently, Zhang's group has developed dual-enzymatic biosensor for the determination of total cholesterol and glucose in serum using poly thionine as a mediator.[30] Raba's group has reported an amperometric rotating biosensor for the determination of total cholesterol using soluble redox mediator.[31] The biosensing of uric acid has been demonstrated using redox mediators based on phenothiazine and phenazine.[32,33] Willner's group has extensively worked in the development of amperometric biosensors for the sensing of glucose, lactate, etc., using wired enzymes, metal nanoparticles, and molecular assemblies.[34−37] Very recently, Karyakin's group has shown the mediating capability of membrane-bound unsubstituted phenothiazine in the biosensing of glucose.[11]

Graphene oxide (GO) is an electronically hybrid material having both sp^2 and sp^3 carbon. The functionalized GO has low background current and improved electron transport properties than unfunctionalized GO and is a suitable candidate for the fabrication of biosensing devices.[38,39] The existence of −OH, −COOH and epoxide on the carbon framework pave a way for its rational functionalization. Such functionalization protocols can be used to manipulate the structure and controls its electronic properties. The covalent or noncovalent functionalization of GO with redox mediator, enzyme, etc. is very promising in the development of electrochemical platforms for electroanalytical applications.[40] Rationally functionalized GO with redox mediators of low redox potential can serve as a versatile biosensing platform for the amperometric sensing of bioanalytes. Functionalization of GO would essentially alter the interlayer spacing[41,42] without changing its chemical integrity, and hence a favorable electron transfer can be expected. The redox enzymes can be easily immobilized on the surface of GO either by chemical coupling or by physical adsorption. The immobilized enzymes/biological recognition elements retain their original activity and can effectively partake in the enzymatic events. Herein we describe the rational redox wiring of Fc units with GO backbone, their electrochemical properties, and the development of integrated biosensing platforms for total cholesterol, uric acid, and glucose. The biosensing approach is based on the mediated bioelectrocatalytic oxidation of analytes by the rationally functionalized GO and the immobilized enzymes. It is demonstrated for the first time that Fc-GO can be a potential candidate for the development of electrochemical biosensors. The Fc-GO efficiently mediates the oxidation of these analytes in the presence of oxidase enzymes.

EXPERIMENTAL PROCEDURES

Reagents and Materials. Graphite, ferrocenecarboxylic acid (FCA), 1,3-diaminopropane (DAP), 1,6-diaminohexane (DAH), 1,9-diaminononane (DAN), N-(3-dimethylaminopropyl)-N-ethylcarbodiimide hydrochloride (EDC), 1-hydroxy benzotriazole (HOBt), N,N-diisopropylethylamine (DIPEA), nafion (5 wt % solution in lower aliphatic alcohol), glucose, uric acid, cholesterol, cholesteryl stearate, ascorbic acid, glucose oxidase (GOx) (from *Aspergillus niger*, 125 units/mg), uricase (UOx) (from *Candida* sp, 4.6 units/mg), cholesterol oxidase (ChOx) (from *Streptomyces* sp., 54 units/mg), and cholesterol esterase (ChEt) (from *Pseudomonas fluorescens*, 13.16 units/mg) were obtained from Sigma-Aldrich and used as received. All other chemicals used in this investigation were of analytical grade (99.9%). Phosphate buffer solution (PBS, 0.1 M) of pH 7.2 was used as supporting electrolyte for all voltammetric and amperometric measurements. All the solutions used in this investigation were prepared with Millipore water (Milli-Q system).

Instrumentation. Fourier transform infrared spectroscopic (FTIR) measurements were performed with Perkin-Elmer FTIR spectrophotometer RX1. KBr pellet was used to prepare the samples for FTIR measurements. All the voltammetric and amperometric measurements were carried out with CHI643B electrochemical analyzer attached to a Faraday cage/current booster (CH Instruments, Austin, TX). X-ray diffraction (XRD) analysis was carried out with a Panalytical high resolution XRD-1, PW 3040/60 unit using Cu target. Powder samples were directly used for the XRD measurements. The UV−visible spectral measurements were carried out with CARY 5000 UV−vis-NIR spectrophotometer. X-ray photoelectron spectroscopy (XPS) measurements were performed with PHI 5000 VersaProbe II scanning XPS microprobe (ULVAC-PHI, inc.) using the energy source Al ($K\alpha$, $h\nu$ = 1486.6 eV). The spectra were analyzed using casaXPS software. Transmission electron microscopic (TEM) measurements were performed with Analytical TEM (FEI-TECNAI G2 20S-TWIN) instruments operating at 200 kV. Energy-dispersive X-ray spectroscopic (EDX) measurement was performed with FEI TECNAI-G2−20S-TWIN instruments with EDAX-EDS attachments (Model No. 942409761751, Standard-2). Carbon-coated copper grid (Pelco International, USA) was used for the sample preparation. All the experiments were performed with screen printed electrodes (SPEs, Dropsens, Spain) with 50 μL of electrolyte. The SPE is equipped with a carbon working (4 mm diameter) and counter and a silver reference electrodes. The SPE was connected to the potentiostat using a DRP-DSC connector (Dropsens, Spain). Electrochemical impedance spectroscopic (EIS) measurements were carried out with Autolab potentiostat-galvanostat (302N) in 0.1 M PBS (pH 7.2) containing 5 mM $[Fe(CN)_6]^{3-/4-}$ as a redox probe by applying an alternating current voltage of 10 mV amplitude and the frequency range was 1×10^{-2} to 1×10^5 Hz. A two-compartment three-electrode cell with a glassy carbon working electrode (GCE), a platinum wire auxiliary electrode and an Ag/AgCl (3 M KCl) reference electrode was used for EIS measurements.

Synthesis of GO and Fc-GO. GO was synthesized according to modified Hummer's method[43,44] by the exfoliation of graphite. Briefly, 50 mL of concentrated H_2SO_4 was slowly added to a mixture of graphite powder (1 g) and $NaNO_3$ (1 g) in a 500 mL round-bottom flask at 0 °C. Solid $KMnO_4$ (6 g) was added to the reaction vessel and the mixture was stirred continuously for 1 h at room temperature. Water (200 mL) was slowly added to the mixture and the stirring was continued for another 15 min. Then H_2O_2 solution (30%) was added to the reaction vessel until the gas evolution was ceased. The resulting mixture was centrifuged in an ultra centrifuge to remove unexfoliated

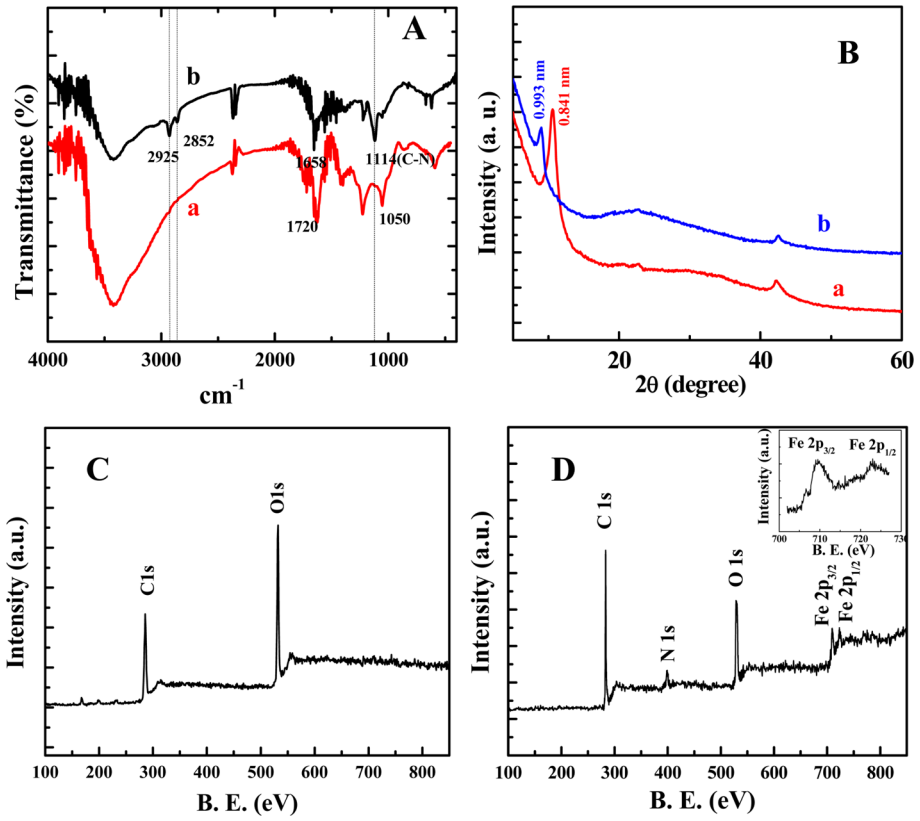

Figure 1. (A) FTIR spectra and (B) XRD profile of (a) GO and (b) Fc-GO with DAN spacer group. (C, D) XPS profiles of GO and Fc-GO, respectively. Inset in D is the Fe 2p spectra.

graphite and oxidizing agents. The residue was then washed repeatedly with aqueous HCl (5%) until the washing solution shows negative test for the presence of sulfate ions with $BaCl_2$ solution. The residue obtained after repeated washing was further washed with copious amount of Millipore water and dried in vacuum to get the yellow brown solid of GO. For the synthesis of Fc-GO, 10 mg of GO was dispersed in 5 mL of DMF, and sonicated for 30 min. FCA (0.01 M) in DMF was then added to this mixture with catalytic amounts of EDC and HOBt (0.005 M each). The reaction mixture was stirred at room temperature for 30 min to activate the acid functionalities of GO and FCA. The sigma spacers (0.01 M) of required length and DIPEA (0.01 M) were added to the reaction mixture[45,46] and stirred for another 12 h at room temperature to obtain the brown-colored Fc-GO (Scheme 1).

Fabrication of Biosensors. SPE was used as conductive substrate for the development of amperometric biosensing platform. First 2 mg of Fc-GO was dispersed in 1 mL of ethanolic Nafion solution (3%) and sonicated for 10 min to get the homogeneous dispersion. An aliquot of the Fc-GO solution (10 μL) was coated over SPE and dried it at room temperature for 1 h. For the fabrication of uric acid and glucose biosensors, 10 μL of the enzyme UOx (10 mg/mL) or GOx (5 mg/mL) in PBS was immobilized over the Fc-GO layer on SPE and was dried at 4 °C for 12 h. For the biosensing of total cholesterol, the enzymes ChOx (10 mg) and ChEt (5 mg) were mixed with 10 μL of PBS (0.01 M) and stored at 4 °C. An aliquot of 5 μL of the resulting enzymes mixture was immobilized on the Fc-GO layer on the SPE and dried it at 4 °C for 12 h. The biosensors were stored at 4 °C when not in use.

RESULTS AND DISCUSSION

Characterization of GO and Fc-GO. The FTIR spectra of GO shows the characteristic stretching frequencies for oxygen containing functional groups such as C═O (1720 cm^{-1}), O−H (3400 cm^{-1}), alkoxy C−O (1050 cm^{-1}), and epoxy C−O (1227 cm^{-1}) (Figure 1A). A new band was observed at 1112 cm^{-1} for Fc-GO and is ascribed for the C−N stretching frequency of amide bond. The stretching frequency (1720 cm^{-1}) corresponding to C═O has shifted to 1658 cm^{-1} after functionalization with Fc due to the amide bond formation. The two new peaks at 2925 and 2852 cm^{-1} for Fc-GO are assigned to the asymmetric and symmetric stretching of methylene groups, respectively (Figure 1A) of the diamine spacer.[47] The XRD profile of GO shows a peak at 2θ = 10.5, which is shifted to 2θ = 8.9 for Fc-GO (Figure 1B), implying the increase in the interlayer spacing from 0.841 to 0.993 nm after functionalization. The effective functionalization essentially increases the spacing between two adjacent layers.[41,42] To further understand the effective functionalization of Fc on GO backbone via diamine spacer, GO and Fc-GO were characterized by XPS measurements (Figure 1). GO shows two peaks at 709.4 and 723.1 eV corresponding to the C 1s and O 1s electrons. On the other hand, Fc-GO shows two new peaks at 709.4 and 723.1 eV, respectively, along with the C 1s and O 1s spectra. The peak at 398.7 eV corresponds to N 1s (Figure 1D). The doublet peaks located at the binding energies of 709.4 and 723.1 eV are assigned for Fe $2p_{3/2}$ and Fe $2p_{1/2}$, respectively (Figure 1D, inset). The appearance of peaks for Fe and N confirm that Fc is successfully wired with GO sheets via diamine sigma spacer. The deconvoluted C 1s spectra for GO shows three peaks located at 284.6, 286.5, and 287.6 eV corresponding to the C═C/C−C, C−O/C═O, and O−C═O functionalities, respectively (see Figure S1 in the Supporting Information). The C 1s spectra for Fc-GO shows two new peaks located at 289.2 eV for N−C═O and 285.9 eV for C−O/C-N functionalities, confirming that Fc units are actually

dx.doi.org/10.1021/am400280u | ACS Appl. Mater. Interfaces 2013, 5, 4791−4798

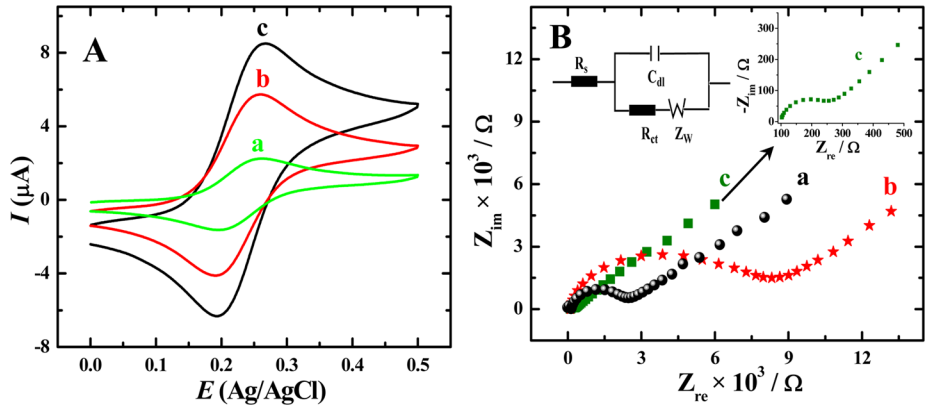

Figure 2. (A) Cyclic voltammetry response of Fc-GO with spacer group (a) DAP, (b) DAH, and (c) DAN in 0.1 M PBS. Scan rate: 50 mV/s. (B) Nyquist plot obtained for (a) bare GCE, (b) GO/GCE, and (c) Fc-GO/GCE in presence of 5 mM $[Fe(CN)_6]^{3-/4}$ in PBS (pH 7.2). The magnified version of curve c and the equivalent circuit are shown in the inset.

attached to GO backbone. The TEM measurements confirm the existence of Fc-GO layer (see Figure S2 in the Supporting Information). The Fc-GO was further characterized by EDX measurements (see Figure S3 in the Supporting Information). The EDX spectra of Fc-GO show four peaks corresponding to C, O, N, and Fe, indicating the presence of Fc units in the GO backbone via diamine sigma spacer; the relative atomic percentage of C, O, N, and Fe were found to be 70.53, 18.24, 7.71, and 3.52% (see Figure S3 in the Supporting Information). The number of Fc units with DAP, DAH and DAN sigma spacers on GO backbone were obtained from spectral measurements (see Figure S4 in the Supporting Information) and were ~0.65, 1.21, and 1.79×10^{20}/mg of GO, respectively.

Electrochemistry of Fc-GO. Figure 2A shows the cyclic voltammetric response of Fc-GO with three different sigma spacers in pH 7.2 (PBS, 0.1 M). Well-defined reversible voltammograms with $E_{1/2}$ value of 0.225−0.228 V were obtained. The peak current linearly scales with sweep rate, suggesting that the redox peak corresponds to a surface confined species (see Figure S5 inset in the Supporting Information). The peak-to-peak separation (ΔE_p) is 67−72 mV and it is independent of scan rate indicating the facile electron transfer reaction. The voltammetric response of Fc-GO with DAN spacer group is highly reversible with an i_p^a/i_p^c ratio of 1 (Table 1). As can be seen from Table 1, a gradual increase in the surface coverage (Γ) of Fc was observed while increasing the spacer length. The increase in the Γ can be explained by considering the coupling efficiency of Fc units with the spacer attached to GO backbone. It is considered that the coupling efficiency of Fc increases while increasing the spacer length, probably due to steric reasons. The amine group of the long chain spacer is easily accessible to ferrocene carboxylic acid for effective coupling. It is apparent from Γ value that the coupling of Fc with DAP spacer is less efficient, as the spacer length is smaller than the other spacers. The voltammetric response due to ferrocene unit on GO backbone did not change upon the repeated cycling between the potential windows of 0.0 to 0.5 V. The heterogeneous electron transfer rate constant (k_s) was calculated for Fc-GO with different spacer length using Laviron approach[48] from the voltammograms obtained at higher scan rate (Table 1). The ΔE_p value at high scan rates is <200 mV and the transfer coefficient α was obtained from the working curve.[48] The k_s value was found to decrease while increasing the spacer length and is in accordance with the literature.[49] The heterogeneous rate constant for the self-assembled monolayer of Fc decreases with increase in the alkane chain length of the monolayer.[49]

Table 1. Electrochemical Parameters Obtained for Fc-GO with Different Spacer Groups

no of carbon in spacer group	ΔE_p (mV)	$E_{1/2}$ (V)	i_p^a (μA)	i_p^a/i_p^c	k_s (s^{-1})	$\Gamma \times 10^{-9}$ (mol/cm^2)
3	67 ± 2	0.227	2.91	1.39	17.6 ± 0.1	0.74 ± 0.2
6	69 ± 2	0.225	5.55	1.16	15.5 ± 0.1	1.76 ± 0.2
9	72 ± 2	0.228	8.55	1.03	14.2 ± 0.1	2.97 ± 0.2

The charge transfer kinetics on Fc-GO-based electrodes was further evaluated by EIS. It may be possible that Fc units on the GO framework can improve the electron transfer kinetics of analytes in solution. In order to examine the charge transfer kinetics, the EIS measurements has been performed using $Fe(CN)_6]^{3-/4-}$ as redox probe. The Nyquist plot and the Randles equivalent circuit used to fit the experimental data are shown in Figure 2B. It is interesting to note that the charge transfer resistance (R_{ct}) on Fc-GO is ~55 times lower than that of the GO (see Table S1 in the Supporting Information), implying that the electrode modified with Fc-GO favor facile electron transfer kinetics. The following three factors can be accounted for such remarkable decrease in the R_{ct} value: (i) the increase in the interlayer spacing, (ii) the electrostatic interaction of unfunctionalized sigma spacer on the GO backbone and (iii) facilitated reaction due to charge transfer between the two redox molecules. The redox marker can easily permeate to the electrode surface when the interlayer spacing is large. As evidenced from the XRD profile, the interlayer spacing in Fc-GO is larger than GO, the redox marker can easily permeate to the electrode surface and hence a favorable electron transfer is anticipated. The contribution from the second factor cannot be ruled out because the R_{ct} value on Fc-GO is much lower than the unmodified GCE (see Table S1 in the Supporting Information). The sigma spacers that do not contain Fc units can be positively charged at neutral pH, as the pK_a of diammines ranges between 9 and 12.[50,51] In such a condition, the negatively charged redox probe can have a favorable electrostatic interaction with the positively charged amine groups and hence a facilitated electrode reaction. The

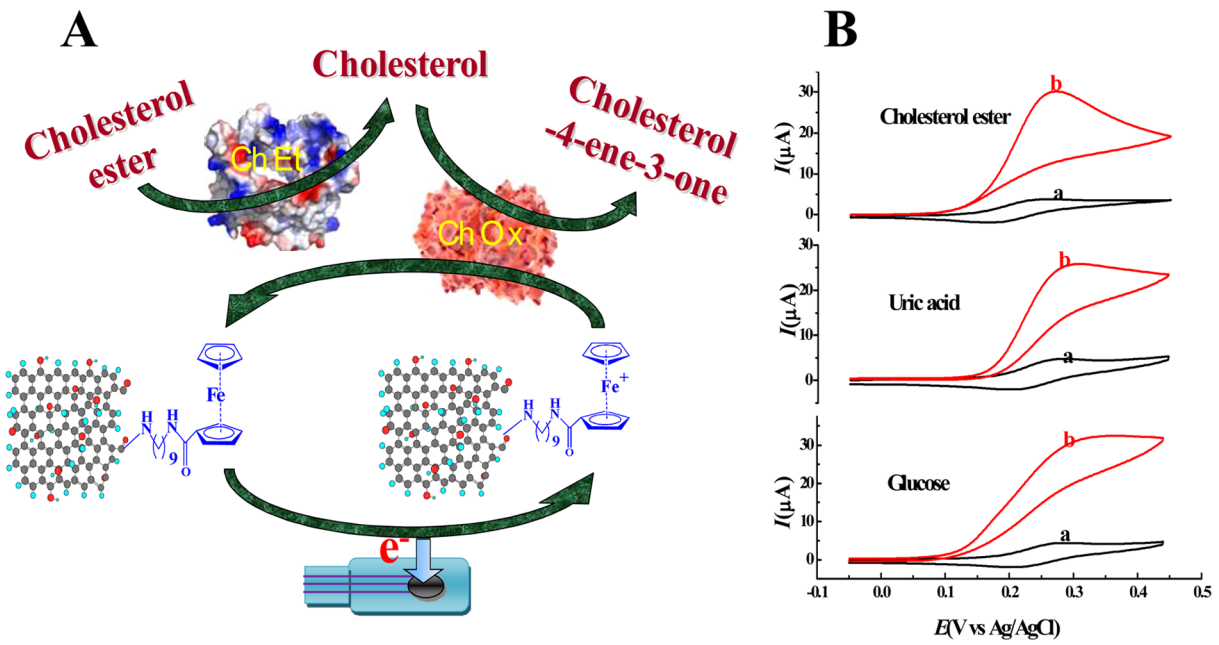

Figure 3. (A) Scheme illustrating the biosensing of cholesterol ester mediated by Fc-GO on SPE. (B) Cyclic voltammetric response of the biosensors toward cholesterol ester, uric acid and glucose in the (a) absence and (b) presence of the respective analytes.

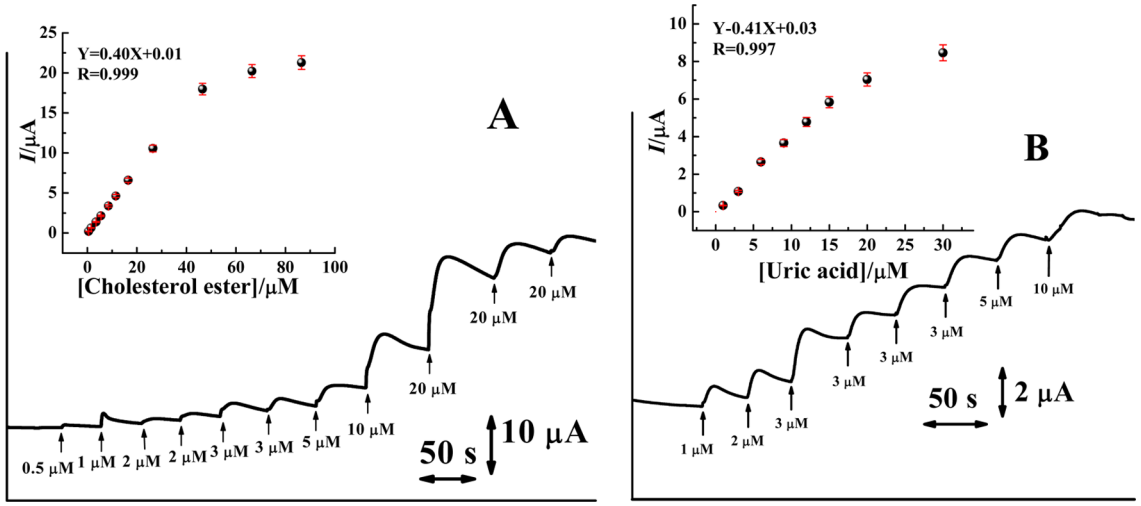

Figure 4. Amperometric response of the (A) cholesterol (total) and (B) uric acid biosensor. Aliquot of respective analytes were injected at regular interval to the supporting electrolyte (PBS, pH 7.2) as indicated by the arrows. The potential of SPE was held at 0.3 V. Inset of each figure shows that the corresponding calibration plot.

facile charge transfer between Fc-GO and $Fe(CN)_6^{3-}$ can also decrease the charge transfer resistance, as both have similar $E_{1/2}$ value.

Bioelectrocatalytic Oxidation of Cholesterol, Uric Acid, and Glucose. The main focus of this investigation is to develop integrated biosensing platform for total cholesterol, uric acid and glucose in serum samples. The biosensing platforms were developed by integrating the redox enzymes and Fc-GO with SPE. Figure 3A depicts the biosensing approach employed for the sensing of cholesterol. In the development of cholesterol biosensor, enzymes cholesterol esterase and cholesterol oxidase were used as >80% of cholesterol in human serum exist in the form of ester. Cholesterol esterase can hydrolyze the ester and cholesterol oxidase can catalyze the oxidation of cholesterol. On the other hand, uric acid and glucose can be directly quantified using enzymes UOx and GOx, respectively. The surface-bound Fc can mediate the electron transfer event. Figure 3B is the bioelectrocatalytic response of the integrated biosensing platform toward the analytes. In the absence of any analytes, the biosensor shows reversible voltammetric response as discussed earlier. A dramatic enhancement in the anodic peak with a concomitant disappearance of the cathodic peak was observed upon injection of analytes, indicating the strong bioelectrocatalytic effect of Fc-GO. The absence of cathodic counterpart in the presence of analytes implies that all the oxidized form of Fc is consumed in the bioelectrocatalytic event. A gradual increase in the peak current was observed while increasing the concentration of the analyte and attained saturation at high concentration, as expected for Michaels-Menten enzyme kinetics. The Fc-GO of the biosensor could successfully communicate with the redox center of the respective enzymes

dx.doi.org/10.1021/am400280u | ACS Appl. Mater. Interfaces 2013, 5, 4791−4798

Table 2. Analytical Performance of the Biosensors Towards Cholesterol Ester, Uric Acid, and Glucose

substrate	K_M^{app} (mM)	linear range (mM)	dynamic range (mM)	LOD (μM)	sensitivity
cholesterol (total)	1.05	0.0005−0.0465	0.0865	0.1	5.71 ± 0.05 μA/μM/cm^2
uric acid	0.34	0.001−0.02	0.03	0.1	5.85 ± 0.10 μA/μM/cm^2
glucose	1.92	0.2−19.7	29.7	1	20.71 ± 0.10 μA/mM/cm^2

and shuttle the electron transfer event in the bioelectrocatalytic oxidation. It should be mentioned that no increase in the anodic current was noticed in the absence of enzymes and Fc. Both enzyme and Fc-GO are required for the bioelectrocatalytic oxidation of the analytes.

Amperometric Biosensing of Cholesterol. Figure 4A is the amperometric response of cholesterol biosensor. The potential of biosensor was held at 0.3 V and aliquot of cholesterol ester was injected. Fast response was obtained during each injection of the analyte. The response was highly stable and gradual increase in the current was obtained. The amperometric response attained saturation at high concentration of cholesterol (Figure 4 inset). The analytical performance of the biosensor is presented in Table 2. The cholesterol biosensor could respond linearly from 0.5 to 46.5 μM and it has dynamic range from 0.5 to 86.5 μM. The detection limit (S/N = 3) and response time of the sensor was 0.1 μM and 4 s. The sensitivity of the sensor was calculated from the calibration plot (Figure 4 inset) and it was 5.71 ± 0.05 μA/μM/cm^2. The apparent Michaelis−Menten constant (K_M^{app}) is a reflection of the enzymatic affinity and it was calculated from the Lineweaver−Burk plot according to the following equation.

$$\frac{1}{I} = \frac{K_M^{app}}{I_{max}[S]} + \frac{1}{I_{max}}$$

where, I is the reaction velocity, I_{max} is the maximum reaction velocity and [S] is the substrate concentration. The K_M^{app} value was calculated to be 1.05 mM, suggesting the high activity and affinity of cholesterol to the enzymes loaded onto the biosensor. When the biosensor was prepared only with GO and enzymes, no response was observed for the analytes, confirming that ferrocene function as a mediator in the oxidation of analytes. It is worth mentioning here that the analytical performance of the biosensors depends on the length of the spacer group. The amperometric signal toward the analytes increases with increasing the spacer length. The sensitivity of Fc-GO containing DAN as spacer group is larger than the others (see Figure S6 in the Supporting Information). This can be explained by considering the Γ of Fc-GO. As shown in Table 1 the Γ of Fc-GO gradually increases with increasing the spacer length and DAN spacer has large Γ. The biosensing performances of uric acid and glucose biosensors are shown in Table 2, Figure 4B, and Figures S7 and S8 in the Supporting Information.

Stability and Reproducibility of the Biosensors. The operational stability of the biosensor was evaluated by measuring the amperometric response of the analytes continuously. No significant change in the initial signal was observed (see Figure S9 in the Supporting Information). The long-term storage stability of the biosensors was evaluated by measuring its performance for 10 days. Amperometric measurements were performed with the same sensor and the sensor was stored at 4 °C after the measurements. A 5% decrease in the initial current after 3 days and 16% decrease after 10 days of storage were observed (see Figure S10 in the Supporting Information). The reproducibility of the biosensors was examined by preparing five biosensors under identical condition on five different days and the amperometric response was evaluated at identical conditions (see Figure S11 in the Supporting Information). The relative standard deviation (RSD) in the amperometric current was only 3%, signifying the excellent reproducibility of the biosensor for practical purpose.

Interference Study. The coexisting common easily oxidizable analytes such as ascorbate and uric acid in the biological fluids can interfere the biosensing of glucose and cholesterol. Fc is known to mediate the oxidation of ascorbate and uric acid in neutral/alkaline pH.[49,52] Voltammetric experiments were performed with Fc-GO in the presence of interfering analytes to examine the interference effect. Interestingly, Fc-GO does not mediate the oxidation of both the analytes even at high concentration (see Figure S12 in the Supporting Information), implying that coexisting these analytes do not interfere the measurement of cholesterol/uric acid/glucose. Ascorbate and uric acid are anionic in neutral pH and they could experience electrostatic repulsion due to the presence of negatively charged Nafion in the biosensing platform. The electrostatic repulsion prevents the easy approach of these interfering analytes to the biosensor surface.

Real Sample Analysis. To examine the versatility of the biosensors for practical applications, we collected three different serum samples from B. C. Roy Technology Hospital, IIT Kharagpur, and quantified the concentration of total cholesterol, uric acid, and glucose using our integrated biosensors. Five independent measurements were performed with each sample and the RSD in the amperometric current ranges between 1 and 4.5. The analytical performance of the biosensor toward serum samples is summarized in Table 3. To authenticate our method, we quantified the concentration of each analyte by conventional clinical procedures (Trinder method).[53] It involves the use of corresponding of oxidase enzymes, peroxidase, and the color indicating reagents (phenol and 4-

Table 3. Biosensing of Cholesterol (total), Uric Acid, and Glucose in Human Serum Samples

analytes	sample No.	measured with Fc-GO biosensor[a] (mg/dL)	measured by clinical method[b] (mg/dL)	RSD[c] (%)
cholesterol (total)	1	107.0	103	4.12
	2	148.2	145	1.76
	3	111.6	107	1.25
uric acid	1	4.79	4.86	4.35
	2	4.95	5.11	4.90
	3	5.11	5.06	3.52
glucose	1	109.5	106	1.47
	2	111.3	116	4.20
	3	95.1	91	1.09

[a]Average of five independent measurements. [b]Estimated by Trinder method. [c]RSD: obtained from five individual measurements of each samples.

Aminoantipyrine). In the case of total cholesterol measurement, the enzymes ChOx and ChEt along with the color indicating reagents were used. As shown in Table 3 the values obtained with our sensors are in close agreement with those of the clinical method, validating the reliability of our biosensors.

It is worth comparing the performance of our biosensor for cholesterol, uric acid and glucose with the existing mediator-based biosensors. The performance of our biosensor is superior to the existing sensors in terms of detection potential, LOD, sensitivity and linear response (see Table S2 in the Supporting Information). The linear response of the biosensor can be extended further by increasing the enzyme loading. More importantly, the biosensor could successfully quantify the concentration of cholesterol ester, uric acid, and glucose in serum samples.

CONCLUSIONS

We have demonstrated the wiring of Fc redox units with GO and the development of highly sensitive amperometric biosensors for the quantification of clinically important analytes cholesterol, uric acid and glucose using the integrated assembly of functionalized GO and redox enzymes. The Fc-GO undergoes facile electron transfer reaction and it could successfully communicate with the redox center of the enzymes. The spacer length plays a key role in the electron transfer reaction. The biosensors are highly stable and they can be used either for a single (disposable) or for repeated measurements. The coexisting interfering analytes in a real sample do not interfere with the amperometric biosensing. The practical application of the biosensors in clinical procedure is demonstrated with human serum samples and the results are excellent agreement with those of clinical method. GO can be an ideal platform for the development of biosensing devices.

ASSOCIATED CONTENT

Supporting Information

Additional figures and table as described in the text. This information is available free of charge via the Internet at http://pubs.acs.org.

AUTHOR INFORMATION

Corresponding Author

*E-mail: crraj@chem.iitkgp.ernet.in. Fax: 91-3222-282522.

Notes

The authors declare no competing financial interest.

ACKNOWLEDGMENTS

R.S.D. is a recipient of the UGC research fellowship. The authors are thankful to B. C. Roy Technology Hospital, IIT Kharagpur for providing human serum samples and the analysis of the samples by clinical laboratory methods.

REFERENCES

(1) Roglic, G.; Enwin, N.; Bennett, P. H.; Mathers, C.; Tuomitehto, J.; Nag, S.; Connolly, V.; King, H. *Diabetes Care* **2005**, *28*, 2130−2135.
(2) Motonaka, J.; Faulkner, L. R. *Anal. Chem.* **1993**, *65*, 3258−3261.
(3) Fox, I. H. *Metabolism* **1981**, *30*, 616−634.
(4) Ullman, B.; Wormsted, M. A.; Cohen, M. B.; Martin, D. W. *Proc. Natl. Acad. Sci. U.S.A.* **1982**, *79*, 5127−5131.
(5) Wang, J. *Chem. Rev.* **2008**, *108*, 814−825 and references cited therein.
(6) Yu, P.; Zhou, H.; Cheng, H.; Qian, Q.; Mao, L. *Anal. Chem.* **2011**, *83*, 5715−5720.
(7) Wang, Z.; Wang, J.; Cheng, H.; Yu, P.; Ye, J.; Mao, L. *Langmuir* **2011**, *27*, 11180−11186.
(8) Wu, J.; Yin, L. *ACS Appl. Mater. Interfaces* **2011**, *3*, 4354−4362.
(9) Yan, Q.; Peng, B.; Su, G.; Cohan, B. E.; Major, T. C.; Meyerhoff, M. E. *Anal. Chem.* **2011**, *83*, 8341−8346.
(10) Wooten, M.; Shim, J. H.; Gorski, W. *Electroanalysis* **2010**, *22*, 1275−1277.
(11) Sekretaryova, A. N.; Vokhmyanina, D. V.; Chulanova, T. O.; Karyakina, E. E.; Karyakin, A. A. *Anal. Chem.* **2012**, *84*, 1220−1223.
(12) Chen, D.; Wang, Q.; Jin, Juan.; Wu, P.; Wang, H.; Yu, S.; Zhang, H.; Cai, C. *Anal. Chem.* **2010**, *82*, 2448−2455.
(13) Wang, Q.; Xu, W.; Wu, P.; Zhang, H.; Cai, C.; Zhao, B. *J. Phys. Chem. B* **2010**, *114*, 12754−12764.
(14) Nakaminami, T.; Kuwabata, S.; Yoneyama, H. *Anal. Chem.* **1997**, *69*, 2367−2372.
(15) Dey, R. S.; Raj, C. R. *J. Phys. Chem. C* **2010**, *114*, 21427−21433.
(16) Heller, A.; Feldman, B. *Chem. Rev.* **2008**, *108*, 2482−2505.
(17) Heller, A.; Feldman, B. *Acc. Chem. Res.* **2010**, *43*, 963−973.
(18) Peng, R.; Zhang, W.; Ran, Q.; Liang, C.; Jing, L.; Ye, S.; Xian, Y. *Langmuir* **2011**, *27*, 2910−2916.
(19) Deng, L.; Liu, Y.; Yang, G.; Shang, L.; Wen, D.; Wang, F.; Xu, Z.; Dong, S. *Biomacromolecules* **2007**, *8*, 2063−2071.
(20) Motonaka, J.; Faulkner, L. R. *Anal. Chem.* **1993**, *65*, 3258−3261.
(21) Zen, J.-M.; Lo, C.-W. *Anal. Chem.* **1996**, *68*, 2635−2640.
(22) Yamamoto, K.; Zeng, H.; Shen, Y.; Ahmed, M. M.; Kato, T. *Talanta* **2005**, *66*, 1175−1180.
(23) Jiang, L.; Liu, H.; Liu, J.; Yang, Q.; Cai, X. *J. Electroanal. Chem.* **2008**, *619*−*620*, 11−16.
(24) Qiu, J.-D.; Zhou, W.-M.; Guo, J.; Wang, R.; Liang, R.-P. *Anal. Biochem.* **2009**, *385*, 264−269.
(25) D'Costa, E. J.; Higgins, I. J.; Turner, A. P. F. *Biosensors* **1986**, *2*, 71−87.
(26) Merchant, S. A.; Tran, Tu O.; Meredith, M. T.; Cline, T. C.; Glatzhofer, D. T.; Schmidtke, D. W. *Langmuir* **2009**, *25*, 7736−7742.
(27) Merchant, S. A.; Meredith, M. T.; Tran, T. O.; Brunski, D. B.; Johnson, M. B.; Glatzhofer, D. T.; Schmidtke, D. W. *J. Phys. Chem. C* **2010**, *114*, 11627−11634.
(28) Liang, R.-P.; Fan, L.-X.; Wang, R.; Qiu, J.-D. *Electroanalysis* **2009**, *21*, 1685−1691.
(29) Scampicchio, M.; Arecchi, A.; Lawrence, N. S.; Mannino, S. *Sens. Actuators, B* **2010**, *145*, 394−397.
(30) Huang, Q.; An, Y.; Tang, L.; Jiang, X.; Chen, H.; Bi, W.; Wang, Z.; Zhang, W. *Anal. Chim. Acta* **2011**, *707*, 135−141.
(31) Salinas, E.; Rivero, V.; Torriero, A. A. J.; Benuzzi, D.; Sanz, M. I.; Raba, J. *Talanta* **2006**, *70*, 244−250.
(32) Nakaminami, T.; Ito, S-i.; Kuwabata, S.; Yoneyama, H. *Anal. Chem.* **1999**, *71*, 4278−4283.
(33) Chen, D.; Wang, Qian.; Jin, J.; Wu, P.; Wang, H.; Yu, S.; Zhang, Hui.; Cai, C. *Anal. Chem.* **2010**, *82*, 2448−2455.
(34) Willner, I.; Baron, R.; Willner, B. *Biosens. Bioelectron.* **2007**, *22*, 1841−1852.
(35) Willner, I.; Katz, E. *Angew. Chem., Int. Ed.* **2000**, *39*, 1180−1218 and references cited therein.
(36) Baron, R.; Willner, B.; Willner, I. *Chem. Commun.* **2007**, 323−332 and references cited therein.
(37) Zayats, M.; Kharitonov, A. B.; Katz, E.; Bückmann, A. F.; Willner, I. *Biosens. Bioelectron.* **2000**, *5*, 671−680.
(38) Li, J.; Guo, S.; Zhai, Y.; Wang, E. *Anal. Chim. Acta* **2009**, *649*, 196.
(39) Zhou, M.; Zhai, Y. M.; Dong, S. *Anal. Chem.* **2009**, *81*, 5603.
(40) Fan, L.; Zhang, Q.; Wang, K.; Li, F.; Niu, L. *J. Mater. Chem.* **2012**, *22*, 6165−6170.
(41) Collins, W. R.; Lewandowski, W.; Schmois, E.; Walish, J.; Swager, T. M. *Angew. Chem., Int. Ed.* **2011**, *50*, 8848−8852.
(42) Herrera-Alonso, M.; Abdala, A. A.; McAllister, M. J.; Aksay, I. A.; Prud'homme, R. K. *Langmuir* **2007**, *23*, 10644−10649.
(43) Hummers, W.; Offeman, R. *J. Am. Chem. Soc.* **1958**, *80*, 1339−1339.

(44) Kovtyukhova, N. I.; Ollivier, P. J.; Martin, B. R.; Mallouk, T. E.; Chizhik, S. A.; Buzaneva, E. V.; Gorchinskiy, A. D. *Chem. Mater.* **1999**, *11*, 771−778.
(45) Hayashi, Y.; Kinoshita, Y.; Hidaka, K.; Kiso, A.; Uchibori, H.; Kimura, T.; Kiso, Y. J. *Org. Chem.* **2001**, *66*, 5537−5544.
(46) Han, S.-Y.; Kim, Y.-A. *Tetrahedron* **2004**, *60*, 2447−2467.
(47) Margarita, H.-A.; Ahmed, A. A.; Michael, J. M.; Ilhan, A. A.; Robert, K. P. *Langmuir* **2007**, *23*, 10644−10649.
(48) Laviron, E. *J. Electroanal. Chem.* **1979**, *101*, 19−28.
(49) Kazakevičienė, B.; Valincius, G.; Niaura, G.; Talaikytė, Z.; Kažemėkaitė, M.; Razumas, V.; Plaušinaitis, D.; Teišerskieneė, A.; Lisauskas, V. *Langmuir* **2007**, *23*, 4965−4971.
(50) Potter, M. J.; Gilson, M. K.; McCammont, J. A. *J. Am. Chem. Soc.* **1994**, *116*, 10298−10299.
(51) Tsubaki, K.; Nuruzzaman, M.; Kusumoto, T.; Hayashi, N.; Bin-Gui, W.; Fuji, K. *Org. Lett.* **2001**, *3*, 4071−4073.
(52) Fernández, L.; Carrero, H. *Electrochim. Acta* **2005**, *50*, 1233−1240.
(53) Trinder, P. *Ann. Clin. Biochem.* **1969**, *6*, 24−25.